INTRACEREBRAL HEMORRHAGE DETECTION IN COMPUTED TOMOGRAPHY SCANS THROUGH COST-SENSITIVE MACHINE LEARNING

Rushank Goyal
Betsos
rgoyal@betsos.org

ABSTRACT

Purpose Intracerebral hemorrhage is the most severe form of stroke, with a greater than 75% likelihood of death or severe disability, and half of its mortality occurs in the first 24 hours. The grave nature of intracerebral hemorrhage and the high cost of false negatives in its diagnosis are representative of many medical tasks.

Approach Cost-sensitive machine learning has shown promise in various studies as a method of minimizing unwanted results. In this study, 6 machine learning models were trained on 160 computed tomography brain scans both with and without utility matrices based on penalization, an implementation of cost-sensitive learning.

Results The highest-performing model was the support vector machine, which obtained an accuracy of 97.5%, sensitivity of 95% and specificity of 100% without penalization, and an accuracy of 92.5%, sensitivity of 100% and specificity of 85% with penalization, on a dataset of 40 scans. In both cases, the model outperforms a range of previous work using other techniques despite the small size of, and high heterogeneity in, the dataset.

Conclusion Utility matrices demonstrate strong potential for sensitive yet accurate artificial intelligence techniques in medical contexts and workflows where a reduction of false negatives is crucial.

Keywords Intracerebral hemorrhage · Computed tomography · Artificial intelligence · Cost-sensitive machine learning

1 Introduction

Intracerebral hemorrhage (ICH) is a neurological condition occurring due to the rupture of blood vessels in the brain parenchyma [1]. is the most severe form of stroke, with the chance of death or severe disability exceeding 75% and only 20% of survivors remaining capable of living independently after 1 month [2, 3]. It has an incidence of 24.6 per 100,000 person-years and accounts for 10-15%

of all strokes [4]. An early diagnosis of ICH is also crucial as half of the mortality occurs in the first 24 hours [5]. Computed tomography (CT) scans are currently the preferred non-invasive approach for ICH detection [6]. The diagnosis time for ICH remains very long, reaching 512 minutes in one study, which, coupled with a high misdiagnosis rate of 13.6% as one estimate calculated, makes it a prime candidate for workflow improvement through machine learning [5, 6].

The conditions and characteristics that are specific to medicine must be taken into consideration during the application of machine learning techniques to medical problems such as ICH diagnosis. A primary concern is that false negatives are usually much more costly than false positives [7]. The frequent under-representation of the minority class coupled with the increased emphasis on its correct prediction makes this a challenging problem for artificial intelligence [8].

Taking the disproportionate costs of false negatives into account (more broadly, a technique called cost-sensitive learning) has resulted in positive outcomes in other medical tasks [9–15]

However, there is very little literature on the application of such techniques in hemorrhage diagnosis. Hence, the aim of this research was to test the results of the implementation of cost-sensitive learning (specifically a utility matrix) on ICH classification.

2 Materials and Methods

The data used for the study were obtained under a CC0: Public Domain license, released by Kitamura [16]. The dataset consisted of 200 anonymized, publicly-available images of non-contrast computed tomography (CT) scans (brain window), 100 of which contained instances of intraparenchymal hemorrhage with or without intraventricular extension, and 100 of which did not. A sample of 4 images from the data is shown in Figure 1. Figure 1a and 1b show scans without intracerebral hemorrhage, at the level of the lateral ventricles and third ventricle, respectively. Figure 1c displays a large intracerebral hemorrhage with intraventricular extension. Figure 1d contains a small intracerebral hemorrhage without intraventricular extension.

A trained radiologist confirmed the veracity of these images, and was unable to find any mislabeled images. Thus none of the images was discarded. To obtain the most accurate representation of model performance in real-life clinical scenarios, the images were not augmented in any way. Two datasets were subsequently created: a training dataset with 160 images and a testing dataset with 40 images. Both had equal numbers of hemorrhagic and non-hemorrhagic CT scans. It should be noted that the dataset consisted of images taken from searches on the World Wide Web, hence introducing a high level of heterogeneity due to variations in source machines, patient conditions, scan time, radiation dose, etc. This problem is compounded by the small dataset size, hence the results obtained here are likely to only be conservative estimates of the real potential of the techniques employed [17, 18].

6 machine learning models were chosen for the study. The specific parameter configurations for these models are provided in Table 1, and are important for reproducibility. A random seed of 0 was used in each case. The models were trained using Wolfram Mathematica Desktop Version 12.3.0, making use of the Classify[] function [19].

2.1 Decision Tree

A decision tree is a machine learning model that consists of nodes and branches, and is built using a combination of splitting, stopping and pruning [20]. Combining all of these techniques, while not

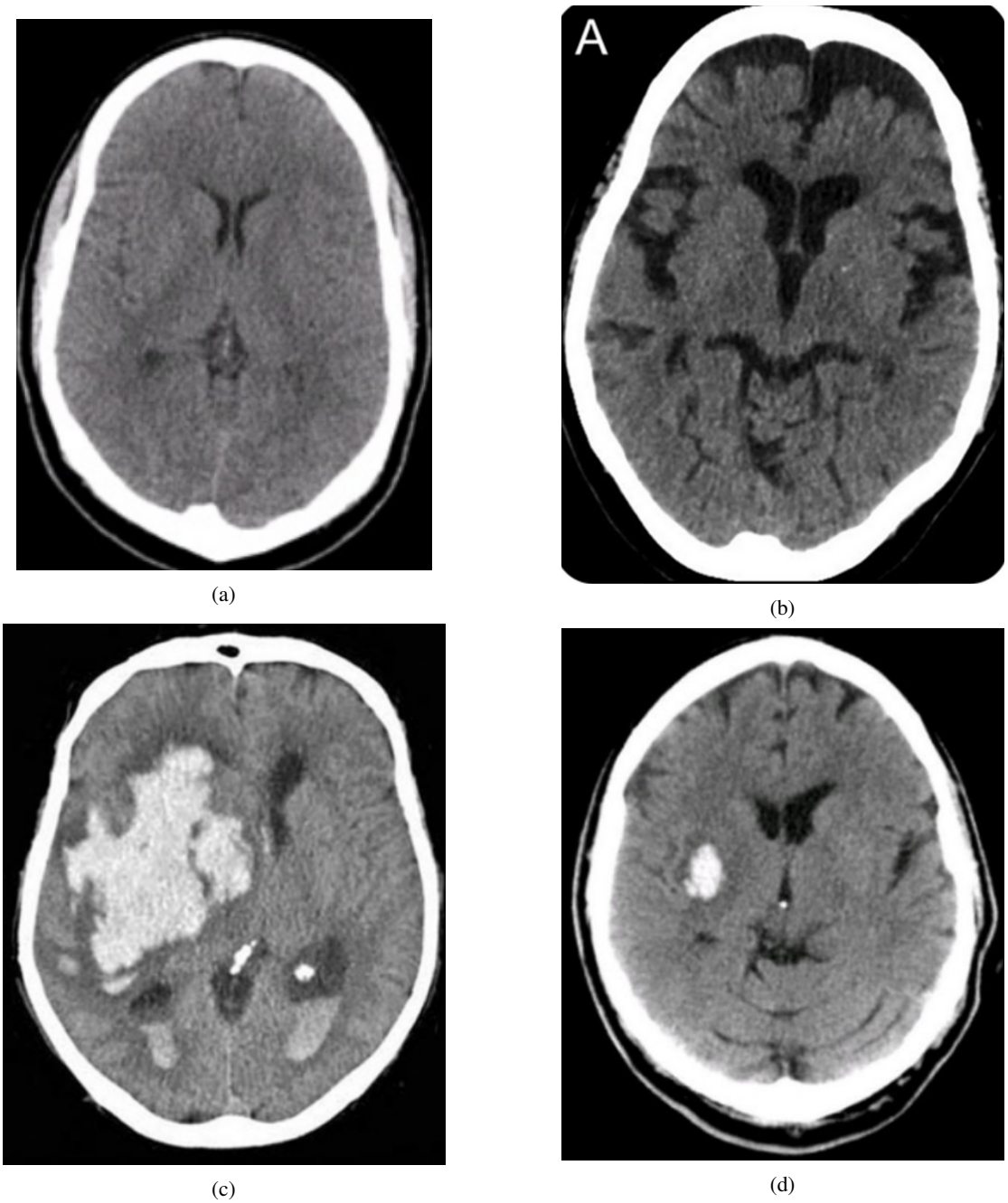

(a) (b) (c) (d)

Figure 1: Sample Dataset Images

guaranteed to result in the theoretically-optimal decision tree – as that would require an exceedingly long time – still results in a highly useful model [21].

2.1.1 Nodes

The root node is the first type of note, and it represents a decision that divides the entire data into two or more subsets. Internal nodes represent more choices that can be used to further split subsets. Eventually, they end in leaf nodes, representing the final result of a series of choices. Any node emanating from another node can be referred to as its child node [20].

2.1.2 Branches

Branches are representations of the outcomes of decisions made by nodes and connect them to their child nodes [20].

2.1.3 Splitting

Both discrete or continuous variables can be used by decision trees to set criteria for different nodes, either internal or root, that are used to split the data into multiple internal or leaf nodes. Decision trees choose between different splitting possibilities using certain measures of the child nodes, such as entropy, Gini index, and information gain, to optimize the splitting choices [20].

2.1.4 Stopping

If allowed to split indefinitely, a decision tree model could achieve 100 % accuracy simply by splitting over and over until each leaf node only had one data sample. However, such a model would be vastly overfitted and would not generalize well to test data. Thus there needs to be a limit (often in the form of maximum depth allowed or minimum size of leaf nodes) [20].

2.1.5 Pruning

There are two types of pruning. Pre-pruning uses multiple-comparison tests to stop the creation of branches that are not statistically significant, whereas post-pruning removes branches from a fully-generated decision tree in a way that increases accuracy on the validation set, which is a special subset of the training data not shown to the model while training [20].

2.2 Random Forest

A random forest, as the name suggests, is a collection of randomized decision trees that is suitable for situations where a simple decision tree could not capture the complexity of the task at hand [22]. The random forest model performs a 'bootstrap' by choosing n times from n decision trees with replacement [23]. The averaging of these predictions is called bagging (short for bootstrap-aggregating) and is a simple way to improve the performance of weak models, which many decision trees are when the task is complex [24].

2.3 Gradient Boosted Trees

Gradient tree boosting constructs an additive model, using decision trees as weak learners to aggregate, similar to the concept of random forests, but it does so sequentially; stochastic gradient descent is then used to minimize a given loss function and optimize the construction of the model as more trees are added [25, 26].

2.4 Nearest Neighbors

The nearest neighbors model is based on the concept that the closest patterns of the data sample in question offer useful information about its classification. Thus the model works by assigning each data point the label of its k closest neighbors, where k is specified manually [27].

2.5 Support Vector Machine

Support vector machines are machine learning models for classification problems [28].

2.5.1 Separating Hyperplane

For *n*-dimensional data, a hyperplane (straight line in a higher-dimensional space) of *n-1* dimensions is used to separate the data into two different groups such that the distance from the clusters is maximized and the hyperplane is 'in the middle', so to speak. This hyperplane also dictates which labels will be assigned to the samples from the test set [28].

2.5.2 Soft Margin

Most datasets, of course, do not have clean boundaries separating different clusters of samples. There will also be outliers, and an optimal model would allow for a certain number of outliers to avoid overfitting while also limiting misclassifications. The soft margin roughly controls the number of examples allowed on the wrong side of the hyperplane as well as their distance from the hyperplane [28].

2.5.3 Kernel Function

A kernel function refers to one or more mathematical operations that project low-dimensional data to a higher-dimensional space called a feature space, with the goal being the easier separation of the example data [29].

2.6 Logistic Regression

Logistic regression is a mathematical model that describes the relationship of a number of features $(X_1, X_2, ..., X_k)$ to a dichotomous result. It makes use of the logistic function, given below [30].

$f(z) = \frac{1}{1+e^{-z}}$

$z = \alpha + \beta_1 X1 + \beta_2 X_2 + ... + \beta_k X_k$

Name	Parameters
Random Forest	FeatureFraction = $\frac{1}{4\sqrt{10}}$, LeafSize = 5, TreeNumber = 50, DistributionSmoothing = 0.5
Decision Tree	DistributionSmoothing = 1, FeatureFraction = 1
Gradient Boosted Trees	BoostingMethod = Gradient, MaxTrainingRounds = 50, LeavesNumber = 13, LearningRate = 0.1, MaxDepth = 6, LeafSize = 15, L1Regularization = 0, L2Regularization = 0
Nearest Neighbors	NeighborsNumber = 5, DistributionSmoothing = 0.5, NearestMethod = Scan
Support Vector Machine	KernelType = RadialBasisFunction, GammaScalingParameter = 0.00113124, PolynomialDegree = 3, SoftMarginParameter = 1, BiasParameter = 1, MulticlassStrategy = OneVersusOne
Logistic Regression	L1Regularization = 0, L2Regularization = 100, OptimizationMethod = LBFGS

Table 1: Parameter Specifications

For the second part of the study, the concept of utility functions was used. A utility function is a mathematical function through which preferences for various outcomes can be quantified [31]. In the case of a utility matrix for classification problems, U_{ij} provides the utility where i is the ground truth and j is the model prediction [32]. It is also referred to as a cost matrix [33].

The utility matrix created for this study is shown in Table 2. The sole difference from the default utility matrix is that false negatives (Row 1, Column 2) now have a utility of -x instead of 0. Subsequent experimentation with different values of x was done and the results were recorded.

Essentially, the models trained using this matrix will have an aversion to false negatives, thus decreasing the number of false negatives at the expense of potentially increasing the number of false positives. The strength of this aversion and subsequent change is quantified by x. A certain amount of trial and error is needed since, for most medical problems, the cost is not certain and needs to be estimated [34]. The cost is context-specific; depending on the workflow where the algorithm is being implemented, the goals for sensitivity and specificity will vary and the cost must be determined accordingly.

In Round 2, the models were re-trained with the same parameters as the previous set, with the only difference being that the value for the 'UtilityFunction' parameter was set to the utility matrix provided in Table 2.

	Hemorrhage	No Hemorrhage
Hemorrhage	1	-x
No Hemorrhage	0	1

Table 2: Utility Matrix

3 Results

The final results for all of the models trained are given in Table 3. The probability histograms for the 3 most accurate models are given in Figure 2. These histograms show the actual-class probability of the 40 test samples. Table 4 lists the results for each of the models after setting their utility function to the matrix given in Table 2, for three values of $-x$. Finally, Figure 3 shows, for the top three models, how their sensitivities and specificities change as the penalty is increased, with 0 being the default penalty that corresponds to Table 3.

	Accuracy	Sensitivity	Specificity
Decision Tree	0.600	0.800	0.400
Random Forest	0.700	0.750	0.650
Gradient Boosted Trees	0.900	0.900	0.900
Nearest Neighbors	0.825	0.700	0.950
Support Vector Machine	0.975	0.950	1.00
Logistic Regression	0.925	0.900	0.950

Table 3: Round 1 Results

According to the data in Table 3, the support vector machine model is the most accurate as well as the most sensitive and specific. Logistic regression and gradient boosted trees score second and third respectively in overall accuracy, though the nearest neighbors model has a higher specificity than gradient boosted trees, coming in second and tied with logistic regression.

Interestingly, while Table 3 shows that the support vector machine is more accurate overall, logistic regression actually appears to be more certain in its predictions, as demonstrated by the difference in the number of samples in the 0.4-0.6 bin. Overall, though, all three of the best-performing models

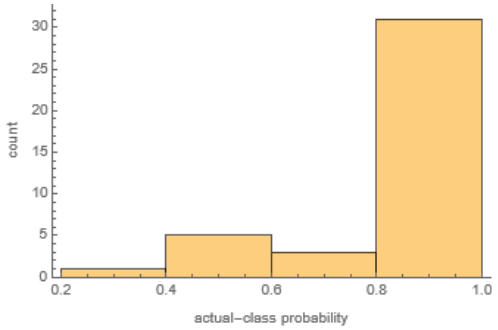

(a) Support Vector Machine

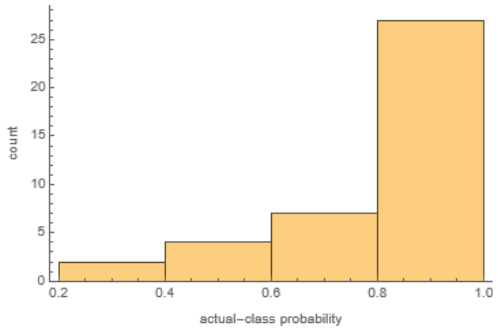

(b) Logistic Regression

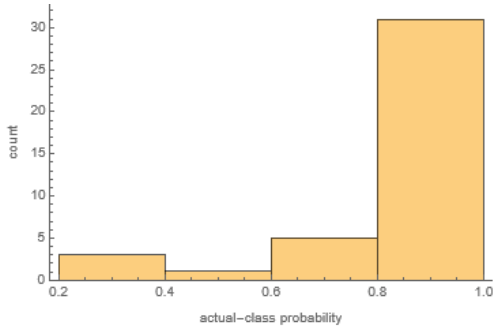

(c) Gradient Boosted Trees

Figure 2: Probability Histograms

seem highly certain in the correct predictions that they are making, as the vast majority of samples fall in the 0.8-1.0 bin.

	Penalty of -1			Penalty of -2			Penalty of -3		
	Acc	Sens	Spec	Acc	Sens	Spec	Acc	Sens	Spec
Decision Tree	0.500	1.00	0	0.500	1.00	0	0.500	1.00	0
Random Forest	0.650	0.900	0.400	0.650	0.900	0.400	0.700	1.00	0.400
Gradient Boosted Trees	0.900	1.00	0.800	0.900	1.00	0.800	0.850	1.00	0.700
Nearest Neighbors	0.800	0.900	0.700	0.800	0.900	0.700	0.625	0.950	0.300
Support Vector Machine	0.925	1.00	0.850	0.925	1.00	0.850	0.900	1.00	0.800
Logistic Regression	0.925	0.950	0.900	0.900	0.950	0.850	0.850	1.00	0.700

Table 4: Round 2 Results

In Table 4, for a penalty of -1, three models give a 100% sensitivity, although for the decision tree that comes at the cost of having a 0% specificity. The support vector machine performs the best, matching the 100% sensitivity of gradient boosted trees. Its specificity of 85% is less than that achieved by logistic regression, though its sensitivity is greater.

The results for a -2 penalty are almost exactly the same, with the only difference being a slightly reduced accuracy for logistic regression.

When the penalty is increased to -3, model performances decrease along the board, except for random forest, which performs better). While the sensitivities for almost all the models are now 100%, they come at the expense of drastically reduced specificities.

Further values of $-x$ were not tested as most model performances had started rapidly deteriorating at a -3 penalty. The random forest, however, might perform better at more negative penalties, based on the observed trends.

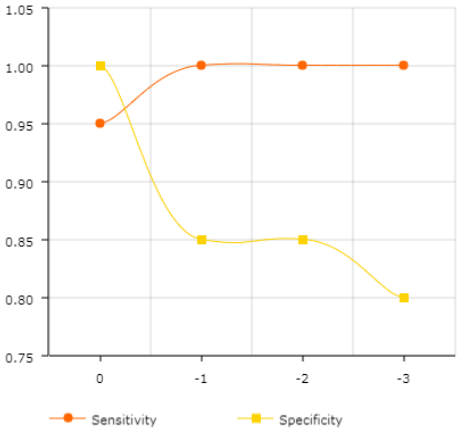

(a) Support Vector Machine

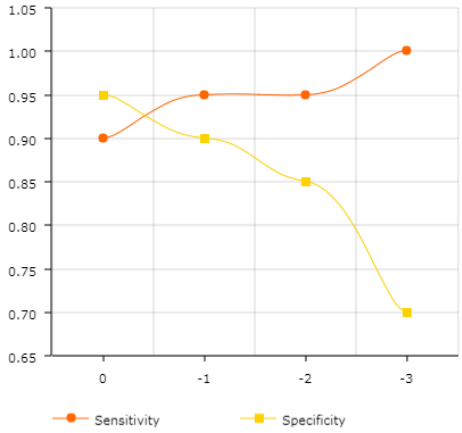

(b) Logistic Regression

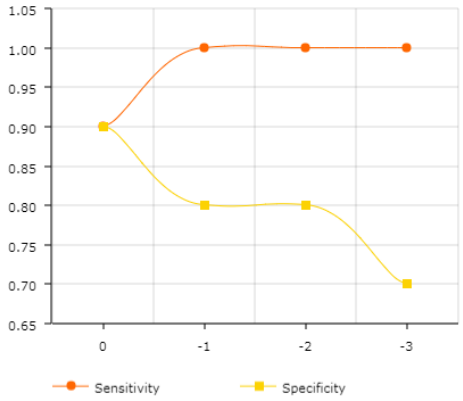

(c) Gradient Boosted Trees

Figure 3: Trends for Sensitivites and Specificities By Penalty

As expected, Figure 3 shows that greater penalties yield reductions in specificity and growth in sensitivity. Though in cases like Figure 3a and Figure 3c, where the sensitivity maxes out early, additional penalties only decrease the specificity. While tweaking the penalties, some changes, such as the one 0.85 to 0.70 in the specificity in Figure 3b, can be quite drastic, making it all the more important to conduct detailed experimentation while determining the penalty.

4 Discussion

The Round 1 results compare favorably to prior studies conducted for ICH identification, especially taking into the account the small training set and heterogeneity in the training data. For instance, work done by Majumdar et al. [35] shows a sensitivity of 81% and specificity of 98%. In one study, the model accuracy of 82%, recall of 89% and precision of 81% remarkably still resulted in a better recall than 2 of the 3 senior radiologists used for benchmarking [36]. More recent research by Dawud et al. [37] resulted in the development of three models, with accuracies of 90%, 92% and

93%. Jnawali et al. [38] performed a study with dataset heterogeneity comparable to ours, although with a considerably larger dataset size of 1.5 million images, and achieved an AUC score of 0.87. A study using 37,000 training samples, also with pronounced heterogeneity in the dataset, obtained an accuracy of 84%, a sensitivity of 70%, and a specificity of 87% [5]. There were also two studies that achieved better accuracies of 99% and one study with an AUC of 0.991 [39–41].

As for cost-sensitive machine learning, only one example could be found for the application of such a technique on intracerebral hemorrhage in prior literature, where the authors ended up achieving an overall sensitivity of 96% and specificity of 95% on a training dataset of 904 cases; the cost in this case was introduced through a modified loss function instead of a utility matrix (used in this study) [42]. A smaller training dataset of 160 images combined with greater heterogeneity likely reduced model performances in this study compared to Lee et al.'s work [17, 18, 42].

The accuracy of the cost-sensitive support vector machine exceeds a number of prior studies' performances. Comparing the accuracy against the array of research mentioned previously, it manages an accuracy greater than the models constructed by Dawud et al., Grewal et al., Arbabshirani et al. and Jnawali et al., while still maintaining a 100% sensitivity [5, 36–38]. As Rane and Warhade pointed out in their literature review, a cost-sensitive algorithm shows great potential as a strategy for more effective diagnosis, and the results confirm this, with the cost-sensitive models demonstrated here outperforming a number of other techniques [43].

Applications Considering the details of utility matrix application and the results it produces, such a type of optimization is suited for a workflow where the artificial intelligence is not working in isolation. Since penalization for false negatives can end up reducing specificities, a further test might become necessary, whether it is a separate algorithm, human clinician(s), or something else. Cost-sensitive learning is ideal in situations where misdiagnosing a positive case could have serious negative impacts, but at the same time the misdiagnosis of a negative case would not cause much inconvenience.

Limitations and Future Research Two main limitations of this study were, as mentioned, the small sample size and high heterogeneity within the dataset. Moreover, due to the nature of the dataset, distinctions based on sex, ethnicity or age weren't possible. Future research that applies cost-sensitive techniques to larger, more standardized datasets, as well as utilizing datasets with details about sex, age, ethicity, etc., could offer greater insights into the advantages and drawbacks of utility matrix-based artificial intelligence algorithms.

Conclusion Clearly, utility matrices have potential as a tool for minimizing unwanted false negatives while still providing accurate overall results. There is a trade-off between sensitivity and specificity, and a suitable value must be chosen after multiple trial and error estimates, but once the ideal penalty has been determined, a cost-sensitive model achieves the given goal better than a more general technique. More work needs to be done on a variety of use cases, not just intracerebral hemorrhage detection, to test the performances of such techniques and their viability in clinical scenarios.

5 Data Availability Statement

The dataset employed was provided under a CC0: Public Domain license by Kitamura [16]. The code for the study can be accessed at `https://github.com/rushankgoyal/cost-sensitive-hemorrhage`

6 Declaration of Conflicts of Interest

No funding was received for conducting this study. The author has no relevant financial or non-financial interests to disclose.

7 Ethical Declarations

This research study was conducted retrospectively using human subject data made available in open access. Ethical approval was not required as confirmed by the institutional review board (IRB) of the Sri Aurobindo Institute of Medical Sciences in Indore, India.

References

[1] Neeraj Badjatia and Jonathan Rosand. Intracerebral Hemorrhage. *Neurologist*, 11(6):311–324, Nov 2005.

[2] Jawed Nawabi, Helge Kniep, Sarah Elsayed, Constanze Friedrich, Peter Sporns, Thilo Rusche, Maik Böhmer, Andrea Morotti, Frieder Schlunk, Lasse Dührsen, Gabriel Broocks, Gerhard Schön, Fanny Quandt, Götz Thomalla, Jens Fiehler, and Uta Hanning. Imaging-Based Outcome Prediction of Acute Intracerebral Hemorrhage. *Transl. Stroke Res.*, pages 1–10, Feb 2021.

[3] Xinghua Xu, Jiashu Zhang, Kai Yang, Qun Wang, Xiaolei Chen, and Bainan Xu. Prognostic prediction of hypertensive intracerebral hemorrhage using CT radiomics and machine learning. *Brain Behav.*, 11(5):e02085, May 2021.

[4] Wendy C. Ziai and J. Ricardo Carhuapoma. Intracerebral Hemorrhage. *CONTINUUM: Lifelong Learning in Neurology*, 24(6):1603, Dec 2018.

[5] Mohammad R. Arbabshirani, Brandon K. Fornwalt, Gino J. Mongelluzzo, Jonathan D. Suever, Brandon D. Geise, Aalpen A. Patel, and Gregory J. Moore. Advanced machine learning in action: identification of intracranial hemorrhage on computed tomography scans of the head with clinical workflow integration - npj Digital Medicine. *npj Digital Med.*, 1(9):1–7, Apr 2018.

[6] Hai Ye, Feng Gao, Youbing Yin, Danfeng Guo, Pengfei Zhao, Yi Lu, Xin Wang, Junjie Bai, Kunlin Cao, Qi Song, Heye Zhang, Wei Chen, Xuejun Guo, and Jun Xia. Precise diagnosis of intracranial hemorrhage and subtypes using a three-dimensional joint convolutional and recurrent neural network. *Eur. Radiol.*, 29(11):6191–6201, Nov 2019.

[7] Claude Sammut and Geoffrey I. Webb. *Encyclopedia of Machine Learning*. xn–3ug : xn–2ug Springer, Mar 2011.

[8] Nguyen Thai-Nghe, Zeno Gantner, and Lars Schmidt-Thieme. Cost-sensitive learning methods for imbalanced data. In *The 2010 International Joint Conference on Neural Networks (IJCNN)*, pages 1–8. IEEE, Jul 2010.

[9] Nontawat Charoenphakdee, Zhenghang Cui, Yivan Zhang, and Masashi Sugiyama. Classification with Rejection Based on Cost-sensitive Classification. In *International Conference on Machine Learning*, pages 1507–1517. PMLR, Jul 2021.

[10] Donovan Fuqua and Talayeh Razzaghi. A cost-sensitive convolution neural network learning for control chart pattern recognition. *Expert Syst. Appl.*, 150:113275, Jul 2020.

[11] Mohammad Khubeb Siddiqui, Xiaodi Huang, Ruben Morales-Menendez, Nasir Hussain, and Khudeja Khatoon. Machine learning based novel cost-sensitive seizure detection classifier for imbalanced EEG data sets. *Int. J. Interact. Des. Manuf.*, 14(4):1491–1509, Dec 2020.

[12] Ali Akbar Septiandri, Aditiawarman, Roy Tjiong, Erlina Burhan, and Anuraj Shankar. Cost-Sensitive Machine Learning Classification for Mass Tuberculosis Verbal Screening. *arXiv*, Nov 2020.

[13] Tianyang Li, Zhongyi Han, Benzheng Wei, Yuanjie Zheng, Yanfei Hong, and Jinyu Cong. Robust Screening of COVID-19 from Chest X-ray via Discriminative Cost-Sensitive Learning. *arXiv*, Apr 2020.

[14] Alberto Freitas, Altamiro Costa-Pereira, and Pavel Brazdil. Cost-Sensitive Decision Trees Applied to Medical Data. In *Data Warehousing and Knowledge Discovery*, pages 303–312. Springer, Berlin, Germany, Sep 2007.

[15] Matjaž Kukar, Igor Kononenko, Ciril Grošelj, Katarina Kralj, and Jure Fettich. Analysing and improving the diagnosis of ischaemic heart disease with machine learning. *Artif. Intell. Med.*, 16(1):25–50, May 1999.

[16] Felipe Kitamura. Head CT - hemorrhage, Aug 2017. [Online; accessed 22. Jul. 2021].

[17] Zoé Lacroix and Terence Critchlow. Compared Evaluation of Scientific Data Management Systems. In *Bioinformatics*, pages 371–391. Morgan Kaufmann, Jan 2003.

[18] Gilbert Lim, Wynne Hsu, Mong Li Lee, Daniel Shu Wei Ting, and Tien Yin Wong. Technical and clinical challenges of A.I. in retinal image analysis. In *Computational Retinal Image Analysis*, pages 445–466. Academic Press, Cambridge, MA, USA, Jan 2019.

[19] Wolfram Research. Classify. `https://reference.wolfram.com/language/ref/Classify.html`, 2021. [Online; accessed 27. Jul. 2021].

[20] Yan-yan Song and Ying L. U. Decision tree methods: applications for classification and prediction. *Shanghai Arch. Psychiatry*, 27(2):130, Apr 2015.

[21] Philip H. Swain and Hans Hauska. The decision tree classifier: Design and potential. *IEEE Trans. Geosci. Electron.*, 15(3):142–147, Jul 1977.

[22] Leo Breiman. Random Forests. *Machine Learning*, 45(1):5–32, Oct 2001.

[23] Gérard Biau and Erwan Scornet. A random forest guided tour. *Test*, 25(2):197–227, Jun 2016.

[24] Leo Breiman. Bagging predictors. *Mach. Learn.*, 24(2):123–140, Aug 1996.

[25] Jerry Ye, Jyh-Herng Chow, Jiang Chen, and Zhaohui Zheng. Stochastic gradient boosted distributed decision trees. In *CIKM '09: Proceedings of the 18th ACM conference on Information and knowledge management*, pages 2061–2064. Association for Computing Machinery, New York, NY, USA, Nov 2009.

[26] Jerome H. Friedman. Greedy function approximation: A gradient boosting machine. *Ann. Stat.*, 29(5):1189–1232, Oct 2001.

[27] Oliver Kramer. K-Nearest Neighbors. In *Dimensionality Reduction with Unsupervised Nearest Neighbors*, pages 13–23. Springer, Berlin, Germany, 2013.

[28] William S. Noble. What is a support vector machine? - Nature Biotechnology. *Nat. Biotechnol.*, 24:1565–1567, Dec 2006.

[29] Shan Suthaharan. Support Vector Machine. In *Machine Learning Models and Algorithms for Big Data Classification*, pages 207–235. Springer, Boston, MA, Boston, MA, USA, 2016.

[30] David G. Kleinbaum and Mitchel Klein. Introduction to Logistic Regression. In *Logistic Regression*, pages 1–39. Springer, New York, NY, New York, NY, USA, Mar 2010.

[31] Stuart J. Russell and Peter Norvig. *Artificial Intelligence: A Modern Approach*. xn–3ug : xn–2ug Prentice Hall, Dec 2002.

[32] Wolfram Research. UtilityFunction. `https://reference.wolfram.com/language/ref/UtilityFunction.html`, 2014. [Online; accessed 26. Jul. 2021].

[33] Charles Elkan. The foundations of cost-sensitive learning. In *IJCAI'01: Proceedings of the 17th international joint conference on Artificial intelligence - Volume 2*, pages 973–978. Morgan Kaufmann Publishers Inc., San Francisco, CA, USA, Aug 2001.

[34] Haomin Wang, Gang Kou, and Yi Peng. Multi-class misclassification cost matrix for credit ratings in peer-to-peer lending. *J. Oper. Res. Soc.*, 72(4):923–934, Apr 2021.

[35] Arjun Majumdar, Laura Brattain, Brian Telfer, Chad Farris, and Jonathan Scalera. Detecting Intracranial Hemorrhage with Deep Learning. *Annu. Int. Conf. IEEE Eng. Med. Biol. Soc.*, 2018:583–587, Jul 2018.

[36] Monika Grewal, Muktabh Mayank Srivastava, Pulkit Kumar, and Srikrishna Varadarajan. RADnet: Radiologist level accuracy using deep learning for hemorrhage detection in CT scans. In *2018 IEEE 15th International Symposium on Biomedical Imaging (ISBI 2018)*, pages 281–284. IEEE, Apr 2018.

[37] Awwal Muhammad Dawud, Kamil Yurtkan, and Huseyin Oztoprak. Application of Deep Learning in Neuroradiology: Brain Haemorrhage Classification Using Transfer Learning. *Comput. Intell. Neurosci.*, 2019:4629859, Jun 2019.

[38] Kamal Jnawali, Mohammad R. Arbabshirani, Navalgund Rao, and M. D. Alpen A. Patel. Deep 3D convolution neural network for CT brain hemorrhage classification. In *Medical Imaging 2018: Computer-Aided Diagnosis*, volume 10575, page 105751C. International Society for Optics and Photonics, Feb 2018.

[39] Annapoorani C. L. Dr. J. Sofia Bobby. Analysis of Intracranial Hemorrhage in Ct Brain Images Using Machine Learning and Deep Learning Algorithm. *Annals of RSCB*, 25(6):13742–13752, Jun 2021.

[40] Mesut Toğaçar, Zafer Cömert, Burhan Ergen, and Ümit Budak. Brain Hemorrhage Detection based on Heat Maps, Autoencoder and CNN Architecture. In *2019 1st International Informatics and Software Engineering Conference (UBMYK)*, pages 1–5. IEEE, Nov 2019.

[41] Weicheng Kuo, Christian xn Hne-tvd, Pratik Mukherjee, Jitendra Malik, and Esther L. Yuh. Expert-level detection of acute intracranial hemorrhage on head computed tomography using deep learning. *Proc. Natl. Acad. Sci. U.S.A.*, 116(45):22737–22745, Nov 2019.

[42] Hyunkwang Lee, Sehyo Yune, Mohammad Mansouri, Myeongchan Kim, Shahein H. Tajmir, Claude E. Guerrier, Sarah A. Ebert, Stuart R. Pomerantz, Javier M. Romero, Shahmir Kamalian, Ramon G. Gonzalez, Michael H. Lev, and Synho Do. An explainable deep-learning algorithm for the detection of acute intracranial haemorrhage from small datasets - Nature Biomedical Engineering. *Nat. Biomed. Eng.*, 3:173–182, Mar 2019.

[43] Harshali Rane and Krishna Warhade. A Survey on Deep Learning for Intracranial Hemorrhage Detection. In *2021 International Conference on Emerging Smart Computing and Informatics (ESCI)*, pages 38–42. IEEE, Mar 2021.